

LOFAR - LOPES (prototype)

<http://www.astro.ru.nl/lopes/>

Radio emission from CRs air showers predicted by Askaryan 1962 and discovered by Jelley et al., 1965 offers the opportunity to carry out neutrino and CR searches from a few up to a few hundred MHz

Already in Haverah Park there were 2 antennas.

The radio emission strength and properties is still highly uncertain hence it is optimal to cross-calibrate with a standard CR experiment (LOPES-Kaskade, Codalema in France is deploying particle detectors, but expensive oscilloscope technology)

Advantages: 100% duty cycle, moderate cost/antenna (many cost data processing) and observations from populated areas

Typical threshold of a purely radio-triggered array: 10^{17} eV

LOFAR: 10000 individual antennas operating in 10-200 MHz range

LOPES: 30 antennas operating in conjunction with Kaskade in Karlsruhe for matching radio signals and air shower events. Data since Jan 2004

LOFAR - LOPES (prototype)

2 mechanisms:

1) Askarian effect: emission of radio Cherenkov radiation from em cascades in particle showers due to build-up of negative charge excess in the em cascade which propagates in a medium at $v > c/n$.

2) in the atmosphere, the emission is dominated by a geomagnetic effect: acceleration of charged particles in Earth's magnetic field

In dense media, such as ice or sand the Askaryan type effect dominates.

Coherent geosynchrotron radiation (Falcke & Gorham, 2003): radiation due to synchrotron pulses from highly relativistic electron-positron pairs gyrating in the Earth's magnetic field. Radiation emitted at low frequencies is expected to be coherent, since the emission wavelength is larger than the air shower pancake (eg $\lambda = 30$ m vs few m pancake thickness at 10 MHz)

Spectral dependence

10^{17} eV vertical air shower at various distances from shower center. Steep decline towards higher frequencies (since coherence diminishes at shorter λ).

The higher the distance from the shower centre, the steeper the spectral dependence of the emission. Hence low frequencies are the most promising regime for observation of CR showers

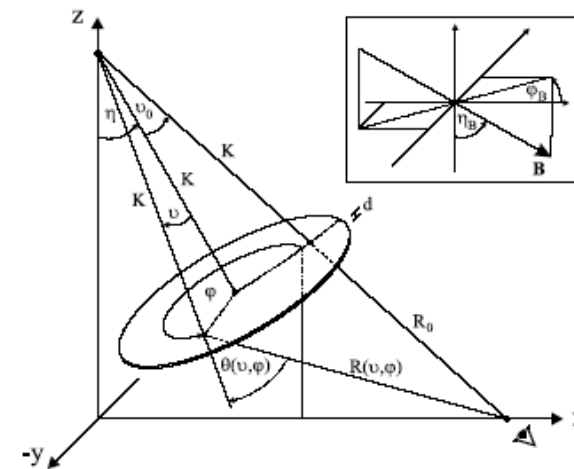
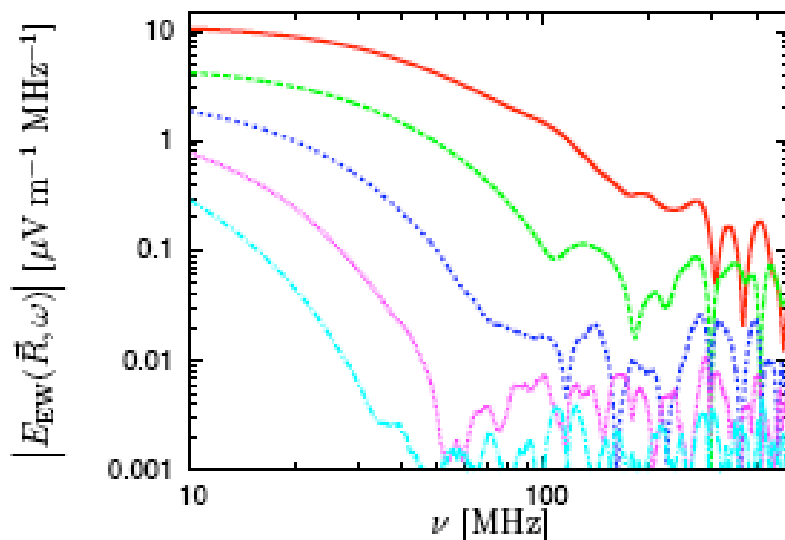


FIGURE 2.8—The geometry for the air shower maximum.

Fig. 1. Spectra of the emission from a vertical 10^{17} eV air shower at various distances to the north. From top to bottom: 20 m, 140 m, 260 m, 380 m and 500 m.

Radial dependence of the radiation

10 MHz component of the E field strength in the linear polarization directions “N-S”, “E-W” and “vertical”. The total field strength is remarkably symmetric in spite of the intrinsic asymmetry of the geomagnetic emission mechanism

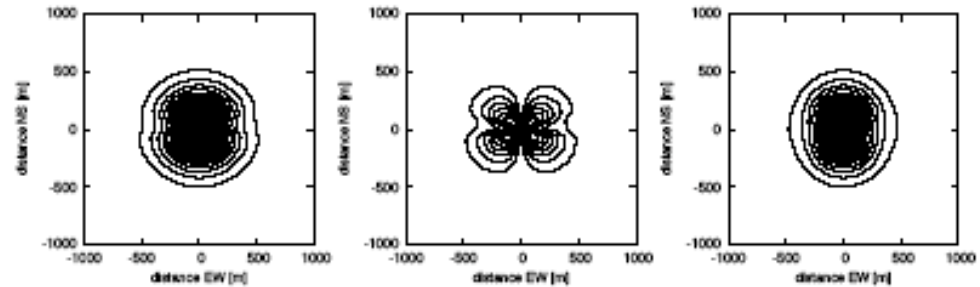


Fig. 3. Contour plots of the 10 MHz field strength for emission from a 10^{17} eV vertical air shower. From left to right: total field strength, north-south polarization component, east-west polarization component. The vertical polarization component (not shown here) does not contain any significant flux. Contour levels are $0.25 \mu\text{V m}^{-1} \text{MHz}^{-1}$ apart.

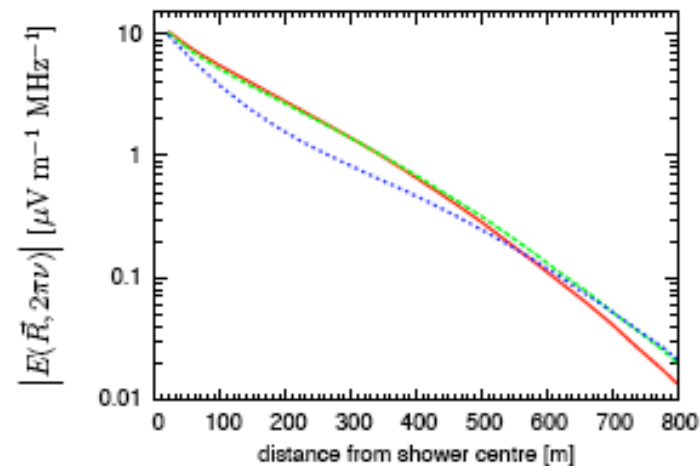


Fig. 4. Radial dependence of the 10 MHz emission from a 10^{17} eV vertical air shower. Solid: to the north, dashed: to the north-west, dotted: to the west.

Radio emission dependence on shower geometry

Radial dependence of the 10 MHz frequency component for air showers coming from the South with different zenith angles. The radial dependence in the North (ie shower axis) becomes much flatter with increasing zenith.

This broadening of the emission pattern is due to the fact that the air shower max for inclined showers is much further away from the ground than for vertical showers. So inclined showers are particularly interesting (also because other techniques as not so good)

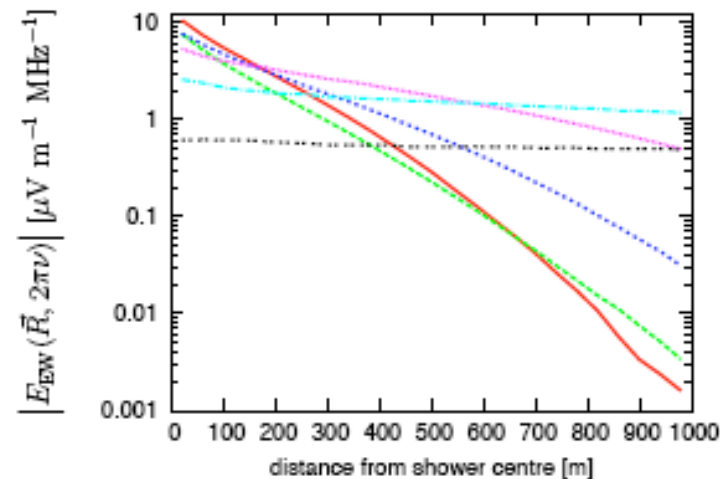


Fig. 8. Dependence of the 10 MHz east-west electric field component emitted by a 10^{17} eV air shower coming from the south for different shower zenith angles as a function of distance to the north. Red/solid: vertical shower, green/dashed: 15°, blue/dotted: 30°, violet/short dotted: 45°, turquoise/dash-dotted: 60°, black/double-dotted: 75° zenith angle.

Radio emission dependence on primary energy

The scaling of the field strength with E_{primary} is approximately $E_{\text{primary}}^{0.96}$

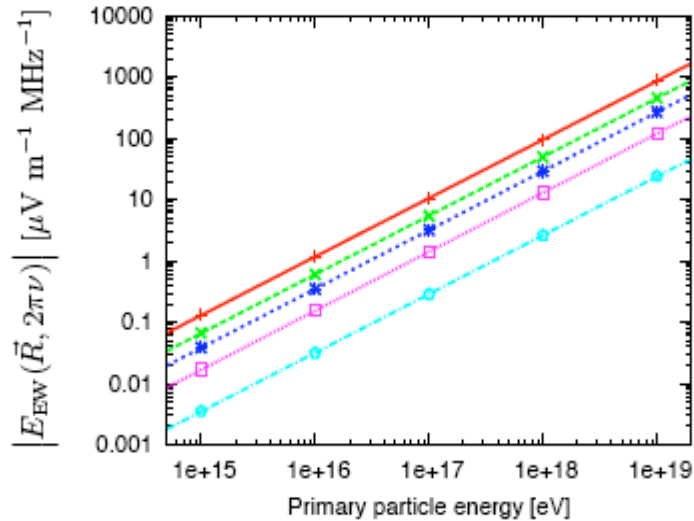


Fig. 16. Scaling of the 10 MHz east-west electric field component emitted by a vertical air shower as a function of primary particle energy E_p . From top to bottom: 20 m, 100 m, 180 m, 300 m and 500 m from the shower center. The data power-law $\propto E_p^{0.96}$.

Keeping X_{max} fixed

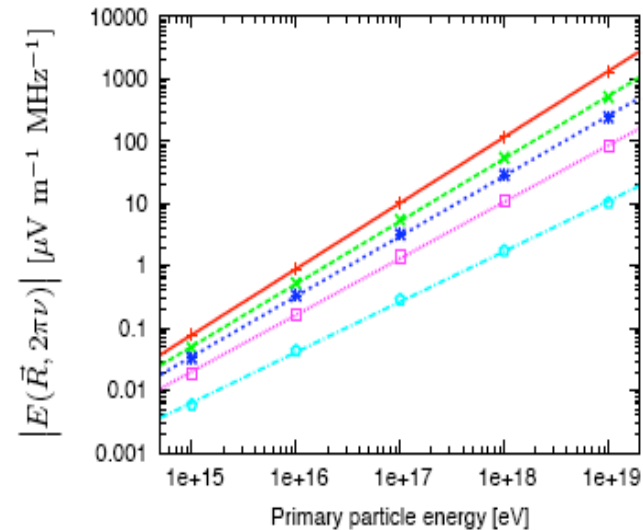


Fig. 21. Scaling of the 10 MHz electric field emitted by a vertical air shower as a function of primary particle energy E_p with appropriately changing depth of shower maximum X_{max} . From top to bottom: 20 m, 100 m, 180 m, 300 m and 500 m to the north from the shower center.

Varying X_{max} appropriately
 increasing X_{max} with E_p leads
 to a radius dependent flattening
 of the energy dependence

LOPES

Detected radio emission from CR air showers at 43-73 MHz with unsurpassed spatial and temporal resolution (Nature 2005). Bandwidth $\Delta\nu = 33$ MHz

Resolution

$$\Delta t = 1 / \Delta\nu = 30 \text{ ns}$$

The CR shower is the bright spot for some 10 ns and the angular resolution is about 2 deg

In LOFAR it will be better

Thanks to the longer interferometric Baselines.

In 6 months 15 events with shower core 70 m from centre of LOPES, $\theta < 45$ deg

And good energy reconstruction

in Kaskade $> 10^{17}$ eV

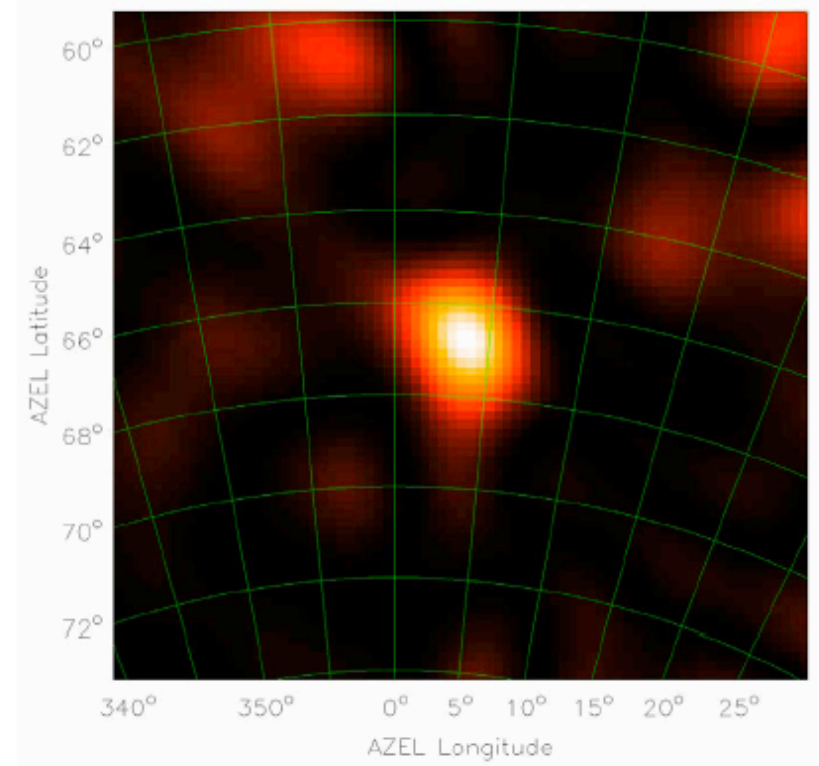


Figure 1 | Radio map of an air shower. For each pixel in the map, we formed a beam in this direction integrated over 12.5 ns and show the resulting electric field intensity. Longitude and latitude give the azimuth and elevation (AZEL) direction (north is to the top, east to the right). The map is focused towards a distance of 2,000 m (fixed curvature radius for each pixel). The cosmic ray event is seen as a bright blob of $2.4^\circ \times 1.8^\circ$ size. Most of the noise in this map is due to interferometer sidelobes caused by the sparse radio array. No image deconvolution has been performed.

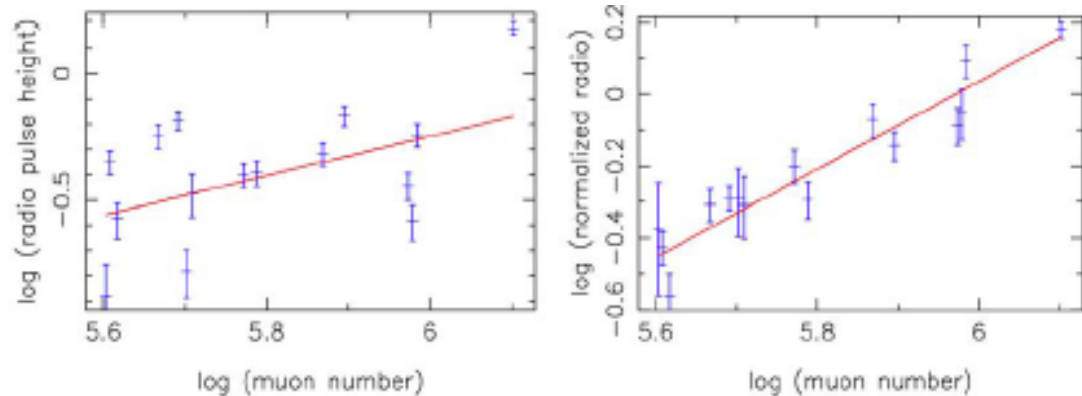
LOPES-Kaskade

Measured radio signal vs number of muons with 10 antennas and 252 Kaskade stations. Antenna set up has max baseline of 125 m. trigger rate 2/min and 3.5 Gbyte/d. Dead time during readout 0.6 s

FWHM of radio pulses
 49 ± 10 ns

$$\varepsilon_{\mu} = \varepsilon / N_{\mu} \propto (1 - \cos \alpha_B)$$

α_b angle between shower axis and magnetic field direction
 This dependence can be used to correct for the geomagnetic angle



$$\varepsilon_{\alpha} \propto N_{\mu}^{1.2 \pm 0.1}, \quad \varepsilon_{\alpha} \propto E_p.$$

Figure 2 | Radio emission as a function of muon number. **a**, The logarithm of the radio pulse height, ε , versus the logarithm of muon number, which has not been corrected for the geomagnetic angle dependence. **b**, As **a** but now the geomagnetic angle dependence is corrected for (ε_{α}). The correlation improves significantly. Solid lines indicate power-law fits. Errors were calculated from the noise in the time series before the pulse plus a nominal 5% error on gain stability. Both errors were added in quadrature. The radio pulse height units are arbitrary.

LOPES-Kaskade

The electric field strength increases linearly with the primary energy due to coherence hence the radio power increases quadratically with E_p

$$\varepsilon_{\alpha} \propto E_p.$$

While shower detectors use the em component that often does not reach ground level a combined radio and muon detector measure signal of muons that always reach the ground. The muon content is larger for iron nucleus compared to p or gamma shower. **Hence the spectrum and composition can be determined by such a combination of detectors.**

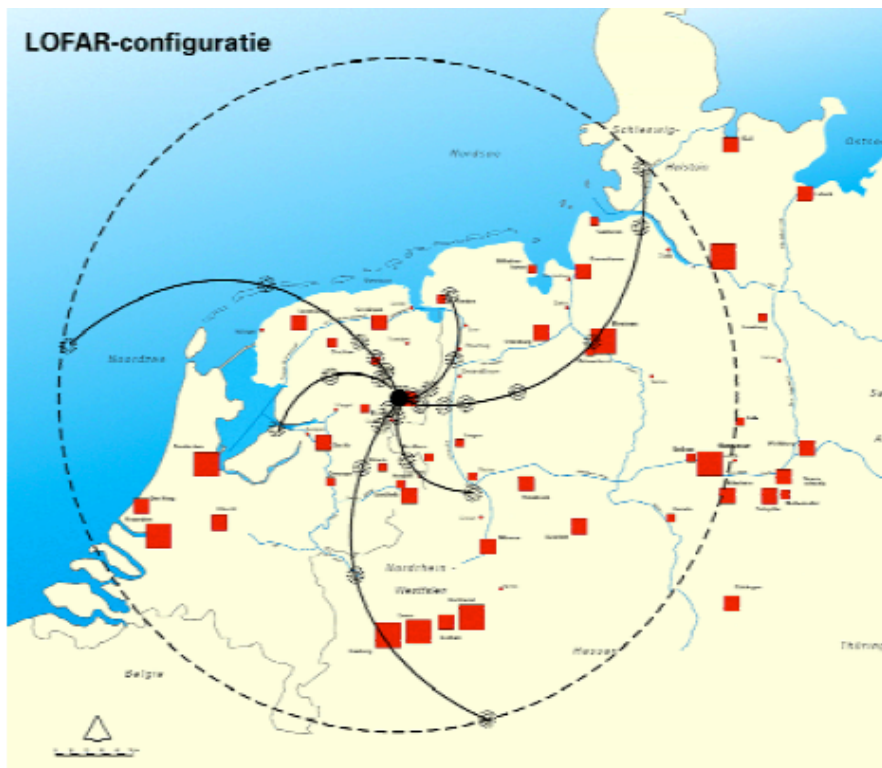
Inclined showers induced by electron neutrinos have small hadronic component Hence the ratio of muon and radio signal will be a tell-tale for electron neutrinos.

Also tau neutrinos can be detected at the horizon where radio antennas are very sensitive. At such inclination no hadronic or gamma showers are expected.

LOFAR

◆ LOFAR

- ⊕ uses **low-cost antennas** and
- ⊕ relies on **broad-band datalinks** and
- ⊕ on **high performance computers** >1000 nodes!!



⊕ LOFAR is a large distributed radiotelescope:

- 100 phased array stations
- Combined in aperture synthesis array
- 13,000 small “LF” antennas
- 13,000 small “HF” tiles
- >20 Tbit/s datanetwork (if full scientific bandwidth)
- >40 Tflop supercomputer
- innovative software systems

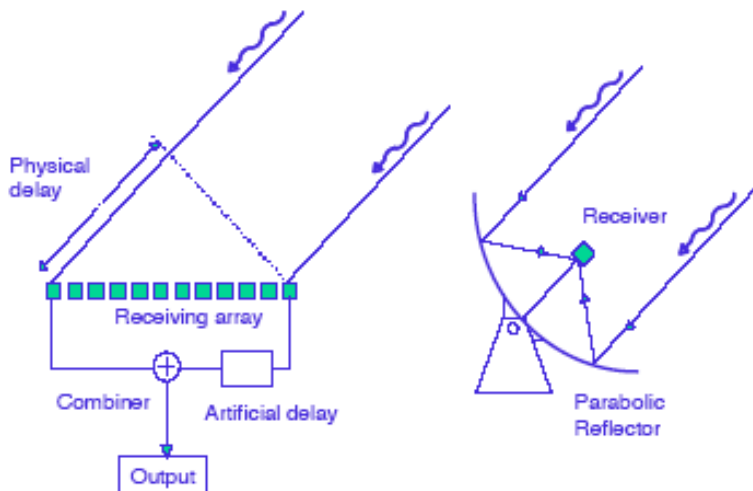
LOFAR antennas

10-90 MHz ... 120-240 MHz



LOFAR is equipped with two types of antennas, optimized for different frequency ranges. Shown is a prototype low-frequency antenna.

Each antenna produces a data rate of 2 Gbits/sec.



Directionality is given by combining signals from various antennas

(phased array) covering

0.03 km² Each station will consist of 100 antennas of each type

The core of diameter 2 km will contain 25% of antennas

